

Design of Array MEMS Vector Vibration Sensor in the Location of Pipeline Internal Inspector

Mengran Liu*, Guojun Zhang, Zeming Jian*, Hong Liu, Xiaopeng Song, Wendong Zhang

Key Laboratory Of Science and Technology on Electronic Test & Measurement, North University of China

*Corresponding author, email: liumengran1991@163.com, zhangguojun1977@nuc.edu.cn, jianzemingx@163.com, liuhongzbdx@163.com, sroc@163.com, wdzhang@nuc.edu

Abstract

In view of the pipeline marking difficult and poor measurement precision, a new-type monolithic integrated array MEMS vector vibration sensor has been put forward. It has overcome the deficiency that present vector acoustic sensor applied in the oil and gas pipeline internal inspector can not be accurate about signal position, and eliminated the port/starboard blur problem. Through ANSYS simulation analysis, it conclude that the array vector vibration sensor has the sensitivity of 2.05mv/pa (-173.8dB, 0dB=1v/ μ pa). The first-order modal is 438 Hz, and the third-order modal is 452 Hz. The resonance frequency of the two sensitive components is respectively 452 Hz and 438 Hz. At the end of this paper, the algorithm that can be used to estimate the azimuth angle detected by the sensor, is given.

Keywords: pipeline internal inspector, above-ground marker, array vibration vector sensor, ANSYS simulation, azimuth estimation

Copyright © 2014 Institute of Advanced Engineering and Science. All rights reserved.

1. Introduction

Pipeline is one of the major mode of transportation of oil and gas resources, which is safe, stable, and economic [1]. In order to guarantee the normal safe operation of pipeline, it is necessary to detect pipeline. Pipeline inspection technology is currently the most widely and most effective pipeline detection method. In order to improve the accuracy of the detector inside, we need to pipeline internal inspector for the ground marker. Currently, there had been some different principle of the ground marker, such as the eddy current methods, magnetic methods and acoustic methods [2-4]. And these markers detection in pipe have achieved better effect on the detection of the pipe. However, nowadays the pipeline is developed toward the direction of large diameter, wall thickness and buried deep, the sensor based on the principle of acoustic detection has become the key point of the development of the technology [5, 6].

The detector inside in the pipe is running under the impetus which is produced by the fluid in the pipe. There have two mainly acoustic signals in the process of running: one is sound signals generated by the friction between internal inspector and pipe wall, the other is impact sound signals between internal inspector and pipeline weld. A large number of the field experiments show that the frequency of the friction acoustic signals is concentrated between 150HZ and 350HZ, while the impact acoustic signals are concentrated between the dozens of HZ. When internal inspector is running in the pipe, the two kinds of acoustic signals will spread around through soil medium. Acoustic signals decay exponentially with the increase of distance in the soil. Due to the effect of attenuation of the soil, the signal will be weaker, the traditional acoustic sensor based on the principle of the vibration acoustic signals detection has no vector. With the acoustic sensor array to detect the position of the internal inspector, however due to the consistency problem of acoustic sensor, so the azimuth estimation precision of the internal detector is not high; and the single vector acoustic sensor also has the port/starboard blur problem (detection range between 0° and 90°). In this paper, there is a new-type array vector vibration sensor with a high sensitivity, which overcomes the shortage of the azimuth estimation in the existing vector sensor array, particularly the defects applied in the location of pipeline internal inspector, and eliminates the port/starboard blur problem.

2. Sensor Structure Design and theoretical Analysis

2.1. Structure Design

In this paper, the structure of array monolithic integrated vibration vector sensor as shown in Figure 1, processing based on SOI material, with a standard pressure resistance type silicon micro mechanical processing technology into four beam arm and the micro column fixed in the center of the four beams of the micro silicon microstructure, which form the sensitive components, and array type vibration vector sensor structure is composed of two such sensitive components. In order to make the two sensitive components of the sensor good consistency, the two sensitive components all the thickness of the beam is $10\mu\text{m}$, length is $1000\mu\text{m}$, width is $120\mu\text{m}$, The radius of the micro column is $100\mu\text{m}$, length is $5000\mu\text{m}$. The arrangement of the four cantilever beam of the two sensitive components is different, and one is the "+" type, the other is a "X" type.

By the diffusion process, four beam arms of each sensitive components has eight equal strain varistor R1, R2, R3, R4, R5, R6, R7, R8, and R9, R10, R11, R12, R13, R14, R15, R16, the distribution of strain varistor connection diagram on the sensors as shown in Figure 2. R1, R2, R3 and R4 connection into the first wheatstone bridge; R5, R6, R7 and R8 connection into the second wheatstone bridge; R9, R10, R11, and R12 connection into the third wheatstone bridge; and R13, R14, R15, R16 connection into the fourth wheatstone bridge. Then a feasible detection circuit is shown in Figure 3.

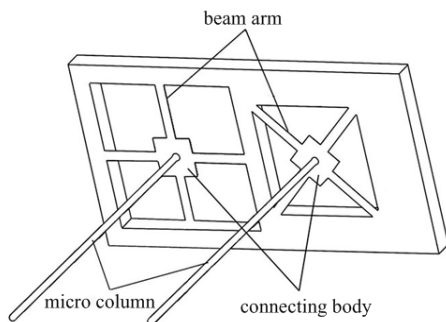


Figure 1. Sensor Structure Diagram

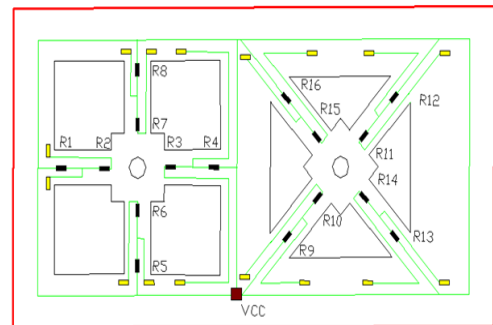


Figure 2. Distribution of Strain Varistor Connection Diagram

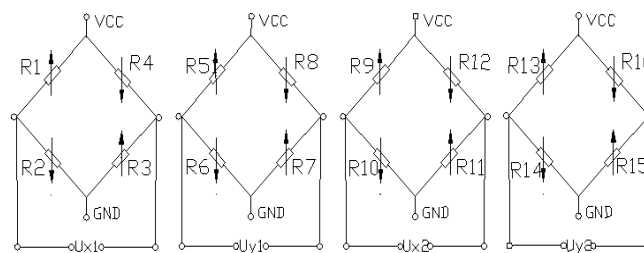


Figure 3. Wheatstone Bridge Circuit Diagram

2.2. Theory Analysis

According to the theoretical knowledge and deduction, the stress $\sigma_{(x)}$ of any point x on single cantilever beam under the action of bending moment $M_{(x)}$ and horizontal force F_H is:

$$\sigma_{(x)} = \pm \frac{L^2 + 3aL - 3x(a+L)}{\frac{2}{3}bt^2(L^2 + 3aL + 3a^2)} M \pm \frac{FH}{bt} \quad (1)$$

Without any stress action (in the first bridge as an example) bridge output voltage can be represented as:

$$V_{out} = \frac{(R_1 R_3) - (R_2 R_4)}{(R_1 + R_2)(R_3 + R_4)} V_{in} = 0 \quad (2)$$

At this point, the bridge is balanced. When there is stress, the pressure sensitive resistance tolerance on the shaft changes, so the output voltage of the bridge is represented as:

$$V_{out} = \frac{(R_1 + \Delta R_1)(R_3 + \Delta R_3) - (R_2 - \Delta R_2)(R_4 - \Delta R_4)}{(R_1 + \Delta R_1 + R_2 - \Delta R_2)(R_3 + \Delta R_3 + R_4 - \Delta R_4)} V_{in} \quad (3)$$

At this point,

$$R_1 = R_2 = R_3 = R_4 = R, \quad \Delta R_1 = \Delta R_2 = \Delta R_3 = \Delta R_4 = \Delta R.$$

Formula (3) can be approximated to:

$$V_{out} = \frac{\Delta R}{R} V_{in} \quad (4)$$

For P type pressure sensitive resistance :

$$\frac{\Delta R}{R} = 71.8 \sigma_1 \times 10^{-11} \quad (5)$$

By the formula (4) and (5):

$$V_{out} = 71.8 \times 10^{-11} \times \sigma_1 \times V_{in} \quad (6)$$

In the formulas: L is the length of the beam (um), b is the width of the beam (um); t is the thickness of the beam (um); a is central connection body half width (um); σ_1 is the maximum stress on sensitive unit corresponding to the direction of X or Y, V_{in} is wheatstone bridge's input voltage [10, 11].

3. Sensor Structure Finite Element Simulation Analysis

Array microstructure finite element model was established by using finite element analysis software ANSYS11. And then we separately carried on the static analysis, modal analysis and harmonic response analysis. The three-dimensional SOLID92 tetrahedron element was used in the process of analysis. The required material properties are shown in Table 1.

Table 1. The Material Properties

Material	Modulus of elasticity(N*m ⁻²)	Poisson's ratio	Density(kg*m ⁻³)
Silicon microstructure	1.65e11	0.278	2330
Cylindrical object	7.4e10	0.17	2320

3.1. The Static Analysis and the Sensor Sensitivity

Constraints are imposed in the base of the array structure. At the same time, 1pa load was applied on micro cylinder y1 positive direction. Then, by defining a path, the stress curve on the array microstructure y1 axis is shown in Figure 4.

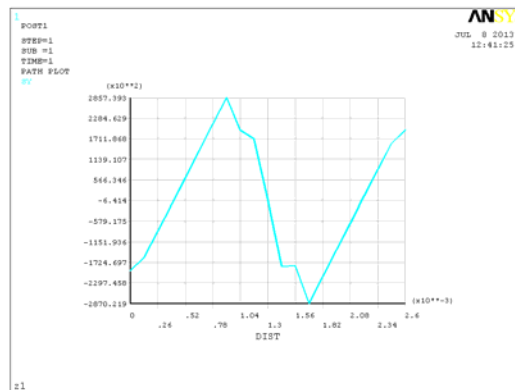


Figure 4. Path Analysis Diagram

The Figure 4 shows that the beam stress is basically linear distribution and the maximum stress appears on both ends of the beam, however, the root of the beam has a beating, so the resistance would better not put there. Therefore the varistor on the beam should be placed in the center away from the root ends $130\mu\text{m}$ [12-15].

The sensitivity of the sensor microstructure can be expressed as the ratio of the output voltage (V_{out}) of the microstructure and the load (F) on the center column. From the formula (6), the sensitivity of the sensitive unit's X axis and Y axis can be represented as:

$$S_{Ax} = S_{Ay} = \frac{V_{out}}{F} = 71.8 \times 10^{-11} \times \sigma_1 \times V_{in} \quad (7)$$

As shown in Figure 4, when 1pa load was applied in micro cylinder y1 positive direction, the sensor maximum stress in y1 axis direction is $\sigma_1 = 285739.3Pa$. Because wheatstone bridge's input voltage is $V_{in} = 10V$, by formula (7), the sensitivity of the sensitive unit's X axis and Y axis is 2.05 mv/pa (173.8 dB).

3.2. Modal Analysis

Modal analysis is generally used to determine the vibration characteristics in the design of the structure or machine parts. The natural frequency of the sensitive components is determined by modal analysis, as shown in Figure 5, and eight modal value of the sensor is shown in Table 2.

Because the fixed silicon base quality around the two sensitive components is different, the natural frequencies of the two sensitive components (the frequency of the first sensitive parts is 452 Hz and the frequency of the second sensitive components is 438 Hz) is different, and there is a certain error.

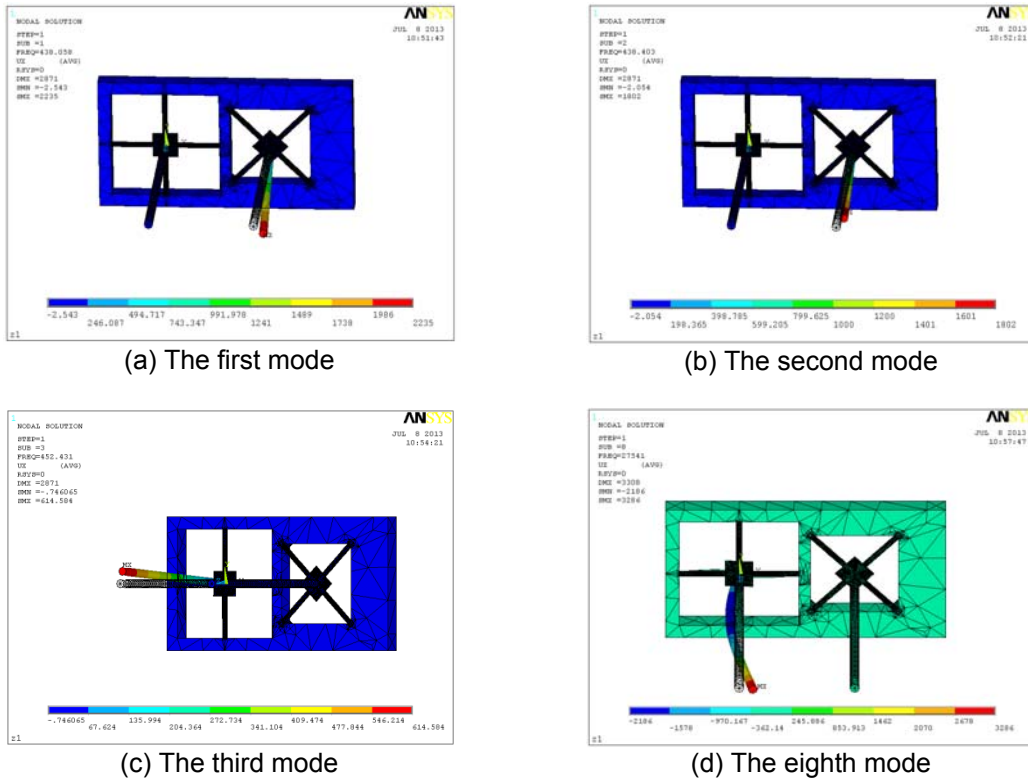


Figure 5. Modal Analysis Diagram

Table 2. Eight Mode Dates of the Sensor

mode	frequency(Hz)
first mode	438
second mode	438
third mode	452
fourth mode	452
fifth mode	1886
sixth mode	2039
seventh mode	27539
eighth mode	27541

3.3. Harmonic Analysis

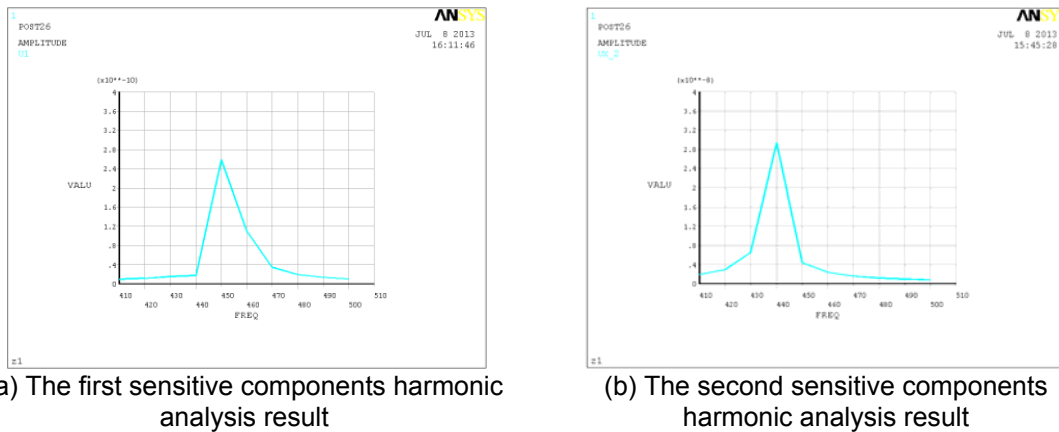


Figure 6. Harmonic Analysis

Harmonic analysis is used to determine the steady-state response of linear structure that sine load changing over time is applied on. And, harmonic analysis can predict the dynamic characteristics of the array microstructure. Therefore, harmonic analysis can be overcome the resonances of array microstructure. Harmonic analysis results of the array microstructure are showed in Figure 6 (the abscissa is the frequency, and the vertical axis is the displacement of y-direction). The results can be seen in Figure 6 that resonant frequencies of sensitive components of the array structure are 452Hz and 438Hz, which consist with the previous analysis results.

4. The Application of the Sensor in the Location of Pipeline Internal Inspector

When the vibration signal is applied to the array vector vibration sensor, θ_1 measured by the first sensitive components and θ_2 measured by the second sensitive components are different in a certain angle, so as to achieve acoustic localization and eliminate the port/starboard blur problem.

When the pipeline inspection gauge moves in the pipeline, it can produce friction sound caused by the detector and the inner wall of pipeline and the crash sound of internal inspector and the weld seams of pipe. The both sound signals can be detected by the array vector vibration sensor. And these two kinds of sound signals through the sensitive component change into voltage signal, so as to achieve the purpose of acoustic localization. In placing the array vector vibration sensor, Cartesian coordinate system is fixed on the ground, and x axis is parallel to the pipe.

If output voltage signal of each sensitive component are V_{x1}, V_{y1} and V_{x2}, V_{y2} . Coordinate of the first sensitive component is considered as a datum (x-y plane) to measure the angle(θ) of the pipeline internal inspector. Angle measured by the first sensitive component is $\theta_1 = \arctan(V_{y1}/V_{x1})(0^\circ < \theta_1 \leq 90^\circ)$, and Angle measured by the second sensitive component is $\theta_2 = \arctan(V_{y2}/V_{x2})(0^\circ < \theta_2 \leq 90^\circ)$. The distance between the sensor and the pipeline internal inspector is much further than the distance between the center of the two sensitive components, so the center of the two sensitive components can be seen at the same origin. Two coordinate systems divide x-y plane into four regions. Array directional diagram is shown in Figure 7.

When $0^\circ < \theta_1 < 45^\circ$, $0^\circ < \theta_2 < 45^\circ$, θ , orientational angle of pipeline internal inspector, is in the region of I and $\theta = \theta_1$.

When $0^\circ < \theta_1 < 45^\circ$, $45^\circ < \theta_2 < 90^\circ$, θ , orientational angle of pipeline internal inspector, is in the region of IV and $\theta = 180^\circ - \theta_1$.

When $45^\circ < \theta_1 < 90^\circ$, $0^\circ < \theta_2 < 45^\circ$, θ , orientational angle of pipeline internal inspector, is in the region of II and $\theta = \theta_1$.

When $45^\circ < \theta_1 < 90^\circ$, $45^\circ < \theta_2 < 90^\circ$, θ , orientational angle of pipeline internal inspector, is in the region of III and $\theta = 180^\circ - \theta_1$.

Estimate direction angle of pipeline internal inspector is shown in Table 3.

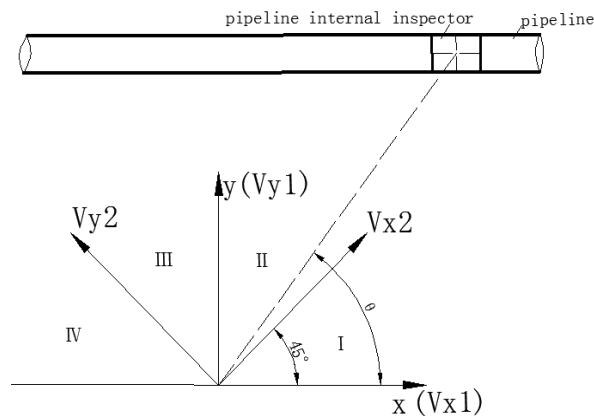


Figure 7. Array Directional Angle Diagram

Table 3. Estimate Direction Angle of the Pipeline Internal Inspector

θ_1	(0° 45°)	45°	(45° 90°)	90°
θ_2	(0° 45°) (45° 90°)	0° 90°	(0° 45°) (45° 90°)	45°
θ	θ_1 180°- θ_1	45° 135°	θ_1 180°- θ_1	90°

4. Conclusion

In view of the serious attenuation of signal emitted by the pipeline internal inspector through the soil medium, and the marking difficult and poor measurement precision, and in order to eliminate the present vector acoustic sensor in judging signal position about pipeline internal inspector port/starboard blur problem, a new-type array MEMS vector vibration sensor has been put forward. Through ANSYS simulation analysis, it conclude that the array vector vibration sensor has the sensitivity of 2.05mv/pa (-173.8dB). The first-order modal is 438Hz, and the third-order modal is 452Hz. The resonance frequency of the two sensitive components is respectively 452Hz and 438Hz, consistent with the first-order modal and the third-order modal. The angles of the two sensitive components are respectively obtained, θ_1 and θ_2 , in the process of measuring the angle of pipeline internal inspector. After analysis and inference, the orientation angle of the pipeline internal inspector can be accurately obtained and the port/starboard blur problem has been eliminated. The list of the specific orientation angle has been given.

References

- [1] Guo Minzhi, Yang JiaYu. Status and development trend of contemporary transportation technology for oil. *China Petroleum and Chemical Industry*. 2004; (7): 16-20.
- [2] Gao Fuqin. Application and development of inner examination technology on pipeline. *Petroleum Planning & Engineering*. 2000; 11(1): 40-41.
- [3] Shen Gongtian, JinG Weike, Zuo Yantian. Review of nondestructive testing technique for buried pipelines. *Nondestructive Testing*. 2006; 28(3): 137-141.
- [4] AC Bruno, R Schifini. New magnetic techniques for inspection and metal-loss assessment of oil pipelines. *Journal of Magnetism and Magnetic Materials*. 2001; 226-230.
- [5] Cui Yao-Yao. Study on the Key Technologies in the Racking and Location System of Pipeline Spection Gauge Based on Acoustic Sensor Arrays. PhD Thesis. Tianjin: Tianjin University. 2011.
- [6] Wu Xiao. Research on Above Ground Marking and Tracking of Oil and Gas Pipeline Internal Inspection Instrument Based on Geophone Array. PhD Thesis. Tianjin: Tianjin University; 2011.
- [7] WU Xiao, JIN Shi-jiu, LI Yi-bo. Above-ground marker system of pipeline internal inspection instrument based on geophone array. *Nanotechnology and Precision Engineering*. 2010; 8(6): 554.
- [8] Mu Linfan, Hui zhenning, Xian zong. Attenuation of sound waves in soil. *Applied Acoustics*. 1995; (01): 19-22.
- [9] GE Xiaoyang, ZHANG Guojun, DU Chunhui. A new MEMS bionic acoustic vector sensor used in above-ground marker of pipeline. *Piezoelectrics & Acoustooptics*. 2012; 34(6): 882-885.
- [10] Chen Shang, Xue Chenyang, Zhang Wendong, Fabrication and testing of a silicon-based piezoresistive two-axis accelerometer. *Nanotechnology and Precision Engineering*. 2008; 6(4): 272-277.
- [11] Chen Shang. Research of a Bionic Vector Hydrophone Based on Silicon. PhD Thesis. Taiyuan: North university of China; 2008.
- [12] Xu Jiao, Zhang Guojun, Shi Guixiong. Advancements in encapsulation of hair vector hydrophone. *Chinese Journal of Sensors and Actuators*. 2011; 24(4): 519-520.
- [13] Liu Linxian, Zhang Guojun, Xu Jiao. Design and test for a double T-shape MEMS bionic vector hydrophone. *Journal of Vibration and Shock*. 2013; 32(2): 130-131.
- [14] Xu Jiao, Li Jun, Zhang Guojun. Design of a novel vector hydrophone based on MEMS. *Piezoelectrics & Acoustooptics*. 2012; 34(1): 90-91.
- [15] Zhang Guojun, Liu Linxian, Zhang Wendong. Performance Research on MEMS Bionic Vector Hydrophone based on "Sandwich"-type package structure. *Sensor letters*. 2012; 10: 712-718.